

Full-F gyrofluid blob dynamics in the tokamak scrape-off-layer

M. Wiesenberger¹, J. Madsen², A. Kendl¹

¹ *Institute for Ion Physics and Applied Physics, University of Innsbruck, Austria*

² *Technical University of Denmark, Department of Physics, Denmark*

Introduction

Radially propagating filaments elongated along magnetic field lines are responsible for a major part of particle density, momentum and energy cross-field transport in the scrape-off-layer (SOL) in Tokamaks[1]. These filaments are widely known as blobs in L-mode operation and ELM filaments in H-mode operation. The particle density amplitude of such structures compared to the background density can be well above unity[1]. Furthermore, the gradient length scale of blobs is comparable to the ion gyroradius. Blobs are born in the vicinity of the last closed flux surface where the background plasma is denser, hotter and has steeper gradients than in the SOL region. Furthermore, in the SOL region the ion temperature is often equal to or higher than the electron temperature.

We present results from simulations of seeded blob convection in the scrape-off-layer of magnetically confined fusion plasmas[2].

Model equations

We restrict ourselves to a simple paradigmatic two-field model which describes the time evolution of the electron particle density n and the ion gyrocenter density N in a simple, quasi-neutral, isothermal, electrostatic plasma in the plane perpendicular to the magnetic field \mathbf{B} at the outboard midplane. We employ a right-handed slab geometry with orthonormal unit vectors $(\hat{\mathbf{x}}, \hat{\mathbf{y}}, \hat{\mathbf{z}})$ with $\hat{\mathbf{z}}$ aligned with the magnetic field and $\hat{\mathbf{x}}$ anti-parallel to the magnetic field gradient. The inverse magnetic field strength is given as $\frac{1}{B} = \frac{1}{B_0} \left(1 + \frac{x}{R}\right)$, where R is the radial distance to the inner edge of the plane at the outboard mid-plane.

$$\frac{\partial n}{\partial t} + \frac{1}{B} \{\phi, n\} + n \mathcal{K}(\phi) - \frac{T_e}{e} \mathcal{K}(n) = \nu \nabla_{\perp}^2 n, \quad (1a)$$

$$\frac{\partial N}{\partial t} + \frac{1}{B} \{\psi, N\} + N \mathcal{K}(\psi) + \frac{T_i}{e} \mathcal{K}(N) = \nu \nabla_{\perp}^2 N, \quad (1b)$$

$$\Gamma_1 N + \nabla \cdot \left(\frac{N}{\Omega B} \nabla_{\perp} \phi \right) = n, \quad (1c)$$

where T_e and T_i denote electron and ion temperature, respectively, ν is the collisional diffusion coefficient, $\Omega = \frac{eB}{m_i}$ and $\nabla_{\perp} = -\hat{\mathbf{z}} \times (\hat{\mathbf{z}} \times \nabla)$. The $\mathbf{E} \times \mathbf{B}$ -advection terms are written in terms of

Poisson brackets which for two arbitrary functions f and g are defined as

$$\{f, g\} = \frac{\partial f}{\partial x} \frac{\partial g}{\partial y} - \frac{\partial f}{\partial y} \frac{\partial g}{\partial x}. \quad (2)$$

The compressibility of the perpendicular fluxes is described by the operator $\mathcal{K} = -\kappa \frac{\partial}{\partial y}$, with $\kappa = 1/(B_0 R)$.

Ion FLR effects appear in the quasi-neutrality constraint Eq. (1c) and in the generalized ion $\mathbf{E} \times \mathbf{B}$ -velocity explicitly through the Padé approximant $\Gamma_1 = (1 - \frac{1}{2}\rho_i^2 \Delta)^{-1}$ to the gyroaveraging operator, where $\rho_i = \sqrt{\frac{T_i}{m_i \Omega_0^2}}$ denotes the thermal ion gyroradius with the constant ion gyrofrequency $\Omega_0 = eB_0/m_i$. The FLR corrected electric potential is $\psi := \Gamma_1 \phi - \frac{m}{2q} \left(\frac{\nabla_{\perp} \phi}{B} \right)^2$.

Energy conservation

The energy theorem is derived multiplying the density equations by $T(1 + \ln N) + q\psi$. Integration over the whole volume and assuming boundary terms to vanish yields

$$\frac{d}{dt} \int_D d\mathbf{x} \left[T_e n \ln n + T_i N \ln N + \frac{1}{2} m_i N \left(\frac{\nabla_{\perp} \phi}{B} \right)^2 \right] = \Lambda \quad (3)$$

where Λ represents the losses due to diffusion.

Simulation Results

We present exemplary blob simulations with and without FLR-effects in Figure (1) and (2). The initially Gaussian shaped blob accelerates radially for both cold and warm ions. Two side-arms with a pronounced cap develop afterwards. For warm ions the blob also accelerates poloidally while the cold ion blob retains an up-down symmetry. In the poloidal turn the warm ion blob becomes stretched and separates from its lobes, streaming upwards thereafter.

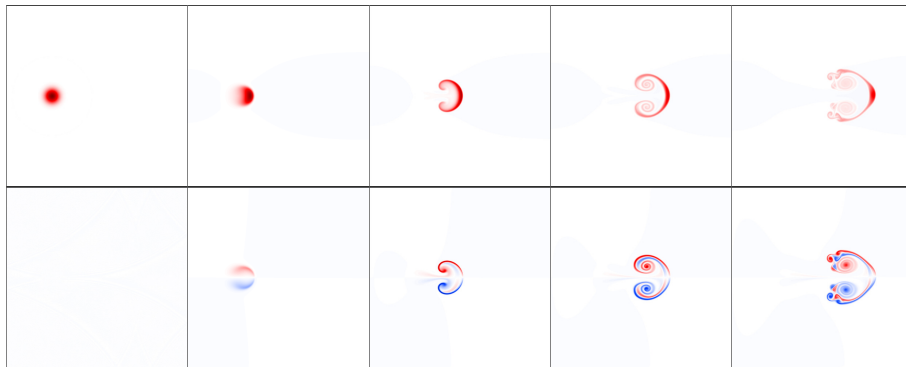


Figure 1: Density n (top) and vorticity $\nabla_{\perp}^2 \phi / B_0$ (bottom) for $T_i = 0$, $\sigma = 10\rho_s$ and $\Delta n = 4n_0$. The first column corresponds to $t = 0$. Going from left to right the time increment is $500\Omega_0^{-1}$. The color scales remains constant. (Taken from Ref. [2])

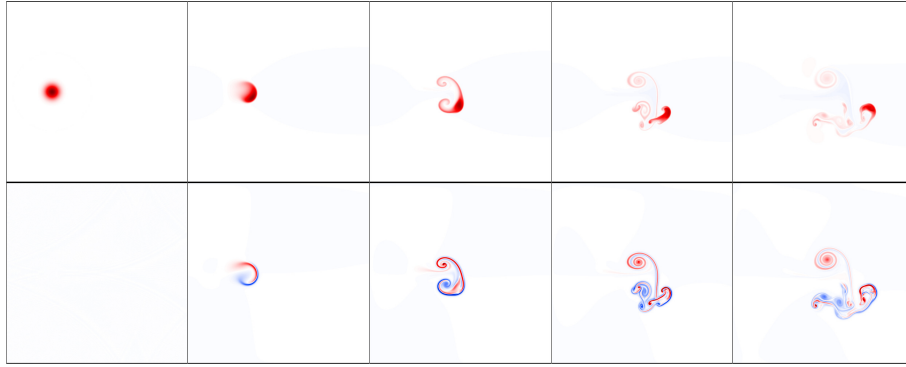


Figure 2: Density n (top) and vorticity $\nabla_{\perp}^2 \phi / B_0$ (bottom) plot for $T_i = 2T_e$, $\sigma = 10\rho_s$ and $\Delta n = 2n_0$. The first column corresponds to $t = 0$. Going from left to right the time increment is $430\Omega_0^{-1}$. The color scales remains constant. (Taken from Ref. [2])

Scanning the parameter range we found that the blob evolution either becomes more mushroom like for low ion temperature and large blob widths or more compact for high ion temperature and small widths. In order to evaluate this observation of blob shapes we use the definition of blob compactness

$$I_C(t) := \frac{\int_D d\mathbf{x} (n(x,y,t) - n_0)h(x,y,t)}{\int_D d\mathbf{x} (n(x,y,0) - n_0)h(x,y,0)}, \quad (4)$$

where h is defined as a Heaviside function

$$h(x,y,t) := \begin{cases} 1 & \text{if } (x - x_{\max}(t))^2 + (y - y_{\max}(t))^2 < \sigma^2, \\ 0 & \text{else.} \end{cases}$$

I_C is a measure for the ability of the blob to retain its form and mass. A small compactness means that the blob has lost most of its initial mass or is spread out over a large area. The mushroom shape should e.g. have a small compactness. A high compactness means that the blob preserves its initial particle density. The high ion temperature blobs should correspondingly have a high compactness. In Fig. 3 we show the blob compactness at time $t = 10c_s \sqrt{\frac{\Delta n}{\sigma R(n_0 + \Delta n)}}$ as a function of the FLR strength, modeled by the control parameter $r = \frac{\rho_i}{\sigma} \frac{\Delta n}{(n_0 + \Delta n)}$. r is the ratio between the ion gyroradius and the initial gradient length scale. We identify two regimes characterized by the FLR-strength. For high values of r the compactness constantly fluctuates around 0.8 for all parameters investigated in this regime. For low values of r the compactness is a factor 2 – 3 times smaller, showing that blob mass in this regime spreads out or diffuses away. The transition between the two regimes happens between $r = 0.06$ and $r = 0.08$.

Furthermore, blobs with very low FLR effects show a significant variation of compactness when amplitude is varied. The smallest values for I_C in our plot can be observed for the low amplitude $\Delta n = 0.1n_0$. When amplitude is increased blob compactness increases as well.

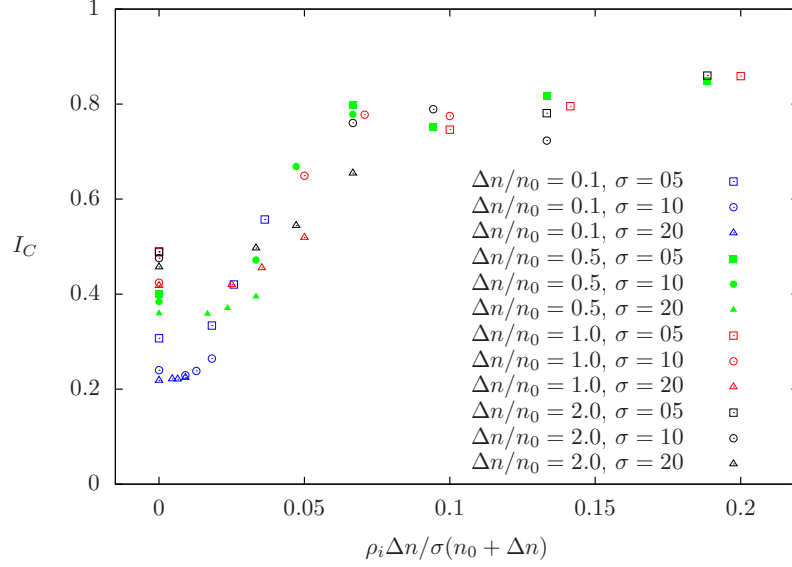


Figure 3: Blob compactness I_C of global blobs as a function of FLR strength at time $t = 10\gamma_{\text{global}}^{-1}$ for various amplitudes and blob widths. (Taken from Ref. [2])

Work in Progress and Outlook

The three-dimensional gyrofluid equations for density N and parallel velocity U derived from the gyrokinetic Vlasov-Maxwell system[3] under the assumption $(\nabla \times \hat{b})_{\parallel} = 0$ read:

$$\partial_t N + \nabla \cdot (N(U\hat{b} + \mathbf{v}_E + \mathbf{v}_C + \mathbf{v}_{\nabla B})) = \Lambda_N \quad (5a)$$

$$\begin{aligned} mN\partial_t U + mN(U\hat{b} + \mathbf{v}_E + \mathbf{v}_C + \mathbf{v}_{\nabla B}) \cdot \nabla U + \nabla \cdot (mNU\mathbf{v}'_C) - mNU(\mathbf{v}_E + \mathbf{v}_{\nabla B}) \cdot \hat{\mathbf{k}} \\ = -\nabla_{\parallel}(NT) - qN\nabla_{\parallel}\psi + \Lambda_U \end{aligned} \quad (5b)$$

We assume an axisymmetric magnetic field and the low- β limit via $\hat{\mathbf{k}} \equiv \hat{b} \cdot \nabla \hat{b} = -\nabla_{\perp} \ln B$. We employ cylindrical coordinates (R, Z, ϕ) and approximate the drift planes as the (R, Z) -planes. The parallel derivative remains, however, exact as $\nabla_{\parallel} \equiv \hat{b} \cdot \nabla$. We use the Lagrangian approach introduced in Ref.[4] in combination with discontinuous Galerkin methods to evaluate this derivative numerically. In the future we want to implement various geometries of the background magnetic field including X-point geometry. Furthermore, an implementation of sheath boundary conditions to model SOL conditions could lead to sophisticated blob simulations.

References

- [1] D.A. D'Ippolito, J.R. Myra, and S.J. Zweben, Phys. Plasmas **18**, 060501 (2011)
- [2] M. Wiesenberger, J. Madsen and A. Kendl, ArXiv:1404.0546 [physics.plasm-ph], (2014)
- [3] J. Madsen et al., Phys. Plasmas **18**, 112504 (2011)
- [4] J. Madsen, Phys. Plasmas, **20**, 072301 (2013)
- [5] F. Hariri and M. Ottaviani, Comput. Phys. Commun., **184**, 11 (2013)